HHS Public Access

Author manuscript

*Clin Cancer Res*. Author manuscript; available in PMC 2016 April 15.

Published in final edited form as:

*Clin Cancer Res*. 2015 April 15; 21(8): 1859–1868. doi:10.1158/1078-0432.CCR-14-1998.

# A translational, pharmacodynamic and pharmacokinetic phase IB clinical study of everolimus in resectable non-small cell lung cancer

**Taofeek K. Owonikoko**[1,2,*], **Suresh S. Ramalingam**[1,2,*], **Daniel L. Miller**[2,3], **Seth D. Force**[2,3], **Gabriel L. Sica**[2,4], **Jennifer Mendel**[2], **Zhengjia Chen**[2,5], **Andre Rogatko**[6], **Mourad Tighiouart**[6], **R. Donald Harvey**[1,2], **Sungjin Kim**[2], **Nabil F. Saba**[1,2], **Allan Pickens**[3], **Madhusmita Behera**[1], **Robert W. Fu**[1], **Michael R. Rossi**[4,7], **William F. Auffermann**[8], **William E. Torres**[8], **Rabih Bechara**[9], **Xingming Deng**[2,7], **Shi-Yong Sun**[1,2], **Haian Fu**[2,10], **Anthony A. Gal**[2,4], and **Fadlo R. Khuri**[1,2,#]

[1]Department of Hematology & Medical Oncology, Emory University

[2]Winship Cancer Institute of Emory University

[3]Department of Surgery, Emory University

[4]Department of Pathology, Emory University

[5]Department of Statistics and Bioinformatics, Rollins School of Public Health, Emory University

[6]Cedars Sinai Medical Center, Los Angeles, California

[7]Department of Radiation Oncology, Emory University

[8]Department of Radiology, Emory University

[9]Division of Interventional Pulmonology, Emory University

[10]Department of Pharmacology, Emory University

## Abstract

**Purpose—**Altered PI3K/mTOR pathway is implicated in lung cancer but mTOR inhibitors have failed to demonstrate efficacy in advanced lung cancer. We studied the pharmacodynamic effects of everolimus in resectable non-small cell lung cancer (NSCLC) to inform further development of these agents in lung cancer.

[#]Corresponding author: Fadlo R. Khuri, MD, Department of Hematology & Medical Oncology, Emory University and Winship Cancer Institute, Suite C3070, 1365 Clifton Road, NE, Atlanta GA, 30322, Tel: 404-778-4250/Fax: 404-778-5520, fkhuri@emory.edu.

[*]Contributed equally and should be considered co-first authors

**Conflicts of interest:**

No significant conflicts reported by the authors.

**Author Contributions:**

Conception and design of study (TKO, SSR, AR, MT, FRK); data collection, analysis and interpretation (TKO, SSR, DLM, SDF, GLS, JM, ZC, AR, MT, RDH, SK, NFS, AP MB, RWF, MRR, WFA, WET, RB, AAG, FRK); manuscript writing (TKO, SSR, DLM, SDF, GLS, JM, ZC, AR, MT, RDH, SK, NFS, AP, MB, MRR, WFA, WET, RB, XD, SS, HF, AAG, FRK); manuscript approval (TKO, SSR, DLM, SDF, GLS, JM, ZC, AR, MT, RDH, SK, NFS, AP, MB, RWF, MRR, WFA, WET, RB, XD, SS, HF, AAG, FRK).

**Experimental Design—**We enrolled 33 patients and obtained baseline tumor biopsy and FDG-PET/CT imaging followed by everolimus treatment (5 or 10 mg daily, up to 28 days), or without intervening treatment for controls. Target modulation by everolimus was quantified *in vivo* and *ex vivo* by comparing metabolic activity on paired PET scans and expression of active phosphorylated forms of mTOR, Akt, S6, eIF4e, p70S6K, 4EBP1 and total Bim protein between pretreatment and post treatment tissue samples.

**Results—**There were 23 patients on the treatment arm and 10 controls; median age 64 years; 22 (67%) were adenocarcinomas. There was a dose-dependent reduction in metabolic activity ($SUV_{max}$: 29.0%, −21%, −24%; p=0.014), tumor size (10.1%, 5.8%, −11.6%; p=0.047), and modulation of S6 (−36.1, −13.7, −77.0; p=0.071) and pS6 (−41.25, −61.57, −47.21; p=0.063) in patients treated in the control, 5mg and 10mg cohorts respectively. Targeted DNA sequencing in all patients along with exome and whole transcriptome RNA-seq in an index patient with hypersensitive tumor was employed to further elucidate the mechanism of everolimus activity.

**Conclusion—**This “window-of-opportunity” study demonstrated measurable, dose-dependent, biologic, metabolic and antitumor activity of everolimus in early stage NSCLC.

### Keywords

Lung cancer; everolimus; biomarker; PET; pharmacodynamic

## Introduction

Altered PI3K /AKT/mTOR pathway signaling is implicated in the development and progression of multiple cancers. It has been identified as an early event in lung carcinogenesis in part based on the high expression of activated mTOR pathway protein members in preneoplastic and cancerous lung lesions relative to normal lung tissue.(1–3) However, clinical trials of mTOR pathway targeted inhibitors administered singly or in combination with standard agents such as docetaxel, pemetrexed, gefitinib and erlotinib in lung cancer patients have achieved only modest efficacy.(4–11) In contrast, demonstrable efficacy of mTOR-targeted agents in breast, kidney and pancreatic neuroendocrine cancers has led to their regulatory approval in these conditions.(12–14) It is currently unknown whether the limited efficacy of mTOR inhibitors in lung cancer compared to other solid tumors reflects a true lack of efficacy, sub-therapeutic dosing regimen or suboptimal clinical trial design in terms of patient selection and endpoints. A better understanding of the biological activity and optimal administration of mTOR inhibitors in lung cancer is therefore necessary if the therapeutic opportunity offered by this class of agents is to be successfully harnessed.

Predictive markers for patient selection and for early determination of long term therapeutic success are important in the development of targeted biologic agents including mTOR inhibitors. Robust evidence from preclinical investigations demonstrated a strong correlation between rapalog exposure and modulation of upstream and downstream mediators of the mTOR signaling cascade, leading to the frequent reliance on changes in the activation status of S6, AKT, p70S6, 4E-BP14E-BP1 and eIF4E as readouts of target engagement and efficient signaling abrogation.(15, 16) Furthermore, metabolic imaging with positron

emission tomography (PET) using $^{18}$F-fluoro-deoxyglucose ($^{18}$F-FDG) and $^{18}$F-fluoro-thymidine radiotracers has been rigorously evaluated in animal models and human subjects and has shown predictive capability for therapeutic efficacy of mTOR inhibitors.(17, 18) These relatively non-invasive tools allow for *in vivo* measurement of biological activity and are useful as early readout of the antiproliferative activity that results eventually in long term efficacy in cancer patients.(17, 18)

The recommended doses for everolimus in early dose finding studies were 10mg daily or 70mg weekly. However, these doses were not defined solely based on toxicity, but on biomarker modulation (S6K) in tumor and surrogate tissues.(19, 20) Based on the wide inter-individual variability in everolimus exposure,(21) it is plausible that a fixed-dose regimen employed in previous lung cancer studies might have been sub-therapeutic in up to a third of patients. Due to concerns about additive toxicities, previous studies of everolimus in lung cancer employed a fixed dose of 5mg, which is lower than the maximum tolerated single agent dose from phase I testing. In order to better characterize the activity of mTOR targeting in lung cancer, we conducted this study to assess the safety and pharmacodynamic effects of everolimus in tumor tissue rather than surrogate tissues both *in vivo* and *ex vivo*. Testing the drug in newly diagnosed, previously untreated patients also allowed for evaluation of drug effect in the native tumor devoid of treatment-induced adaptations. This preoperative window-of-opportunity trial platform uniquely allows for *in vivo* and *ex vivo* assessment of pathway modulation and antitumor effects.

## Materials and Methods

The primary objectives of this phase IB trial were to assess the safety of everolimus in patients with surgically resectable lung cancer and to determine pharmacodynamic (PD) effects of everolimus in previously untreated, surgically resectable, non-small cell lung cancer patients. The safety endpoint was treatment-emergent toxicity graded according to CTCAE version 3 criteria and length of hospital stay post surgery. The PD endpoints included metabolic response on paired FDG-PET scan (defined using PERCIST criteria(22) based on changes in $SUV_{max}$ between baseline and repeat imaging just prior to surgery); to assess the degree of target modulation as indicated by changes in the activated forms of key protein mediators of mTOR pathway signaling including Akt, mTOR, p70S6K, 4E-BP1 and p-S6.

### Eligibility

Patients were eligible if newly diagnosed with non-small cell lung cancer (NSCLC) of all histologies and deemed to be surgically resectable Stage I-IIIA disease. Other eligibility requirements included age ≥ 18 years, ECOG performance status of 0–2, adequate bone marrow function (WBC ≥ 3,000 cells/mm$^3$, ANC ≥ 1,500 cell/mm$^3$, platelets ≥ 100,000 cells/mm$^3$), renal function (creatinine <1.5 X ULN), hepatic function (bilirubin ≤ 1.5 X ULN, SGOT/SGPT ≤ 2.5 X ULN, alkaline phosphatase ≤ 5 X ULN). Specific exclusion factors included inability to swallow pills, known hypersensitivity to everolimus or any of its excipients; pregnancy or breast-feeding; major intercurrent medical, psychiatric or social impairment that would limit compliance with study requirements and chronic treatment with

systemic steroids or other immunosuppressive agent. The study was conducted under a prospective clinical trial protocol approved by the Emory University IRB (IRB00024810). All enrolled patients were recruited through the multidisciplinary thoracic oncology clinics of Emory Clinic of Emory University. All participants provided a written informed consent prior to undergoing any protocol-mandated procedures. The study was registered at www.clinicaltrials.gov (NCT00401778); detailed protocol is available on the clinicaltrials.gov reporter website.

Patient selection for treatment administration: Eligible patients were enrolled concurrently on the active and control arms. Patient preference for a specific arm was entertained until the control cohort was completely filled after which all patients were competitively enrolled on the active treatment arm of the study. (Fig. 1). For safety reason, enrollment into the active treatment group started with the 5mg cohort followed by the 10mg dose cohort in the absence of unanticipated toxicities. Everolimus was self administered by patients at home except on pharmacokinetic samples collection days when the research staff witnessed the drug ingestion prior to sample collection. Patients on the active treatment arm received everolimus daily continuously for three weeks with allowance for an additional week of therapy if necessary to facilitate repeat PET imaging and surgical resection of the tumor, which were mandated to occur within 24 hours of the last dose of everolimus. Patients on the control arm were required to wait for similar amount of time between the baseline and repeat PET scan without receiving any treatment.

## Metabolic Imaging

All patients had baseline imaging in a fasted state with $^{18}$FDG-PET scan and a repeat scan at 3 to 4 weeks later using routine clinical protocol for patient preparation, radiotracer administration and data acquisition. The repeat imaging occurred no longer than 24 hours before surgical resection.

## Pharmacokinetic analysis

Peripheral blood samples for everolimus PK analysis were collected into potassium-ethylene-diamine tetraacetic-acid (EDTA) tubes on days 1, 8 and 21 at 30 minutes before, and 1, 2, 5, 8 and 24 hours following, ingestion of everolimus. Samples were initially stored at 2–8°F during PK collection and subsequently stored within 60 minutes of collection in a −20°F refrigerator, after which all samples were analyzed in a single batch. Following high throughput liquid/liquid extraction, everolimus concentration was measured by a previously validated liquid chromatography (LC)/mass spectrometry (MS) method.(23) The lower limit of quantification was 0.3 ng/mL. Standard non-compartmental analysis of everolimus was performed using WinNonlin Professional software version 5.2 (Pharsight Corporation, St. Louis, Mo) according to the rule of linear trapezoids. Parameters ($C_{max}$, $t_{max}$, AUC) were determined and steady state PK measures on Days 8 and 21 were compared to those on Day 1.

## Pharmacodynamic (PD) assessment of protein expression in paired tumor tissues

Changes in the expression of key signaling proteins in the mTOR/PI3K pathway were determined by immunohistochemistry using previously published protocols and

manufacturers' recommendations for antigen retrieval and antibody dilution along with positive and negative controls. The following primary antibodies were employed at the indicated dilution: S6 (Cell Signaling, Danvers MA Cat#2217) at 1:100 dilution, phospho-S6$^{Ser235/236}$ (Cell Signaling, Danvers MA Cat#2211) at 1:200 dilution, p70S6 Kinase (Cell Signaling, Danvers MA Cat#9202) at 1:100 dilution, phospho-p70S6 Kinase$^{Thr421/Ser424}$ (Cell Signaling, Danvers MA Cat#9204) at 1:100 dilution, Akt (Cell Signaling, Danvers MA Cat#9272) at 1:200 dilution, phospho-Akt$^{Ser473\ (736E11)}$ (Cell Signaling, Danvers MA Cat#3787) at 1:200 dilution, eIF4E (Cell Signaling, Danvers MA Cat#9742) at 1:200 dilution, phospho-eIF4E$^{Ser209}$ (Cell Signaling, Danvers MA Cat#9741) at 1:200 dilution, 4E-BP1 (Cell Signaling, Danvers MA Cat#9452) at 1:200 dilution, phospho-4E-BP1$^{Thr37/46}$ (Cell Signaling, Danvers MA Cat#2855) at 1:200 dilution, mTOR (Cell Signaling, Danvers MA Cat#2972) at 1:200 dilution, phospho-mTOR$^{Ser2448\ (49F9)}$ (Cell Signaling, Danvers MA Cat#2976) at 1:100 dilution, human cytokeratin, clones AE1/AE3, (Dako, Carpinteria, CA cat# M3515) at 1:50 dilution and Bim (Cell Signaling, Danvers MA Cat#2933) at 1:100 dilution. Two investigators assessed protein expression jointly by light microscopy. The degree of expression was assessed by intensity (0, 1+, 2+, 3+) and percentage of cell staining in line with published algorithm.(24) A derivative score (immunoscore) ranging between 0 and 300 was calculated as the product of intensity and percent cell staining.

### Targeted DNA sequencing

SNaPshot multiplex sequencing technique was employed to identify known driver mutations in frequently mutated genes in lung cancer including AKT1 (c.49G>A), BRAF (c.1397G>T, c.1406G>A/C/T, c.1789C>G, c.1799T>A), EGFR (c.2156G>A/C, c.2369C>T, c.2573T>G, c.2582T>A, exon.19.del, exon.20.ins), ERBB2 (ins.A775/exon.20.ins), KRAS (c.181C>A/G, c.182A>C/G/T, c.183A>C/T, c.34G>A/C/T, c.35G>A/C/T, c.37G>A/C/T, c.38G>A/C/T, c.180.181TC>CA), MEK1 (c.167A>C, c.171G>T, c.199G>A), NRAS (c.181C>A/G, c.182A>C/G/T) and PIK3CA (c.1624G>A/C, c.1633G>A/C,c.3140A>G/T). Sample preparation and genetic mutation identification followed previously described methodologies.(25)

### Gene expression profiling using RNA-Seq analysis

Tumor samples from a patient with sarcomatoid variant of NSCLC who achieved complete metabolic response and complete pathologic response in the resected tumor specimen were subjected to detailed genetic analysis to identify potential drivers of this response. Total RNA was isolated from FFPE tumor biopsy and resection specimens using the QIAGEN miRNeasy FFPE kit. Total RNA quality and quantity was determined using the Agilent RNA 6000 Nano kits with the Agilent 2100 Bioanalyzer. RNA-Seq library was generated using NuGen Ovation® kit by AKESOgen (AKESOgen Inc., Norcross, GA). Paired end (100×100) sequencing was performed at Beckman Coulter Genomics using an Illumina HISeq2000 instrument. Data quality was assessed on a minimum of 50 million reads per sample using HTQC and FastQC tools. FASTQ reads were aligned to the human reference build 37/hg19 using TopHat alignment. Gene fusions were identified using TopHat Fusion and differential gene expression was performed with CuffDiff.

### Statistics

The following statistical assumptions were made with regard to study design and sample size estimate. We wanted to guard against intolerable toxicity in more than 3 patients out of 10 treated at each of the 2 doses of everolimus tested in the study. We target the dose such that the probability of intolerable toxicity does not exceed 5%. If four or more patients experienced intolerable toxicity at a given dose, we reject the hypothesis that the probability of DLT does not exceed 5% for that dose. The probability of observing 4 or more DLTs and incorrectly terminating the trial is 0.00547. The planned accrual is at most 32 eligible patients total, with 10–12 patients assigned to receive 5.0 mg/day, 10 patients assigned to 10 mg/day of everolimus and an additional 10 patients accrued to the control arm. Changes between baseline and repeat measurement for mean $SUV_{max}$ and mean anatomic tumor size were compared by t-test and ANOVA. Correlation between metabolic change and tissue based biomarker modulation was assessed by Pearson correlation coefficient test. All analyses were performed using SAS statistical package V9.3 (SAS Institute, Inc., Cary, North Carolina). The significance level was set at 0.05 for all tests without correction for multiple comparisons.

## Results

### Screening, enrolment and baseline characteristics

We screened 45 patients for enrolment from March 2007 through February 2013. Eight patients withdrew consent prior to any protocol-mandated procedure and four were screen failures. Based primarily on patient preference and order of enrolment, we assigned 33 consenting and eligible patients with resectable lung cancer to the control (10 patients) or treatment (everolimus - 5mg daily in 12 patients and 10mg daily in 11 patients) arms. Baseline patient demographics and tumor characteristics are provided in Table 1. Thirty patients (90%) completed all assigned interventions including paired PET scans (at baseline and within 24 hours of surgery), baseline tissue biopsies and resected tumor tissue.

### Safety

Observation for up to 4 weeks without immediate surgical resection did not result in any major untoward effects in patients on the control arm. A single patient in the control group had premature termination of surgery due to intraoperative finding of mediastinal lymph node involvement upstaged the disease stage. The majority of treated patients (17 patients) did not experience any delays on completion of planned interventions and proceeded to surgery within 24 hours of the repeat PET scan. The median and mean time elapsed from end of treatment to surgical resection was 0 and 1 day respectively (range, 0 – 7 days). There was a 7-day delay in planned surgical resection in one patient with persistent treatment-related grade 3 diarrhea. Three patients experienced delays of 2 and 3 days in planned surgery due to logistical difficulties with scheduling, while another patient underwent surgery early due to rapid disease progression after only 10 days of everolimus therapy. All other patients proceeded to surgery as planned. Patients in the treatment arm tolerated everolimus. Preoperative adverse events experienced by patients treated with everolimus were mostly anticipated, grade 1 or 2 on the NCI Common Terminology Criteria for Adverse Events (CTCAE) grading scale and were managed conservatively. These are

summarized by grade and type in Table 2. Notable post-surgical complications considered unrelated to preoperative everolimus therapy included: altered mental status in 2 patients and respiratory failure and prolonged ventilator-dependence in the setting of polymicrobial or methicillin-resistant *Staphylococcus aureus* (MRSA) pneumonia leading to tracheostomy in 3 patients. The median and mean length of hospital stay (LOS) after resection was 5 and 8.6 days respectively (range, 2 – 43 days). The median LOS was 5 days for both treated (range, 3 – 43 days) and control patients (range, 2 – 15 days).

## Everolimus Pharmacokinetics

Whole blood samples collected from 12 patients treated with the 5mg dose and 7 patients treated with the 10mg dose of everolimus were employed for PK characterization. Day 1 and steady-state concentrations are shown in Table 3a. Summary data are reported from steady-state day 8 and 21 values. The median $C_{max}$ at steady state and $AUC_{0-24}$ were dose-proportional, with rapid absorption seen in each group (Fig. 1). There was no significant accumulation at either dose level. Mean half-life in each group was estimated to be 26.5 and 30.3 hours for 5mg and 10mg, respectively. The PK characteristics of everolimus determined using extensive sampling on days 1, 8 and 21 were overall consistent with those previously reported by our group and others.(10, 19)

## Efficacy

**Metabolic Response—**Comparison of the maximum standardized uptake value ($SUV_{max}$) from baseline $^{18}$F-FDG PET/CT scans and the repeat scan just prior to surgery was used to assess metabolic response induced by the two different doses of everolimus compared to the untreated patients. Changes in $SUV_{max}$ are expressed as a percent change of initial $SUV_{max}$). Patients treated with everolimus 5mg and 10mg had a mean reduction of 21% and 24%, respectively, in comparison to a mean increase of 29% in control patients ($p=0.014$); Figure 2A. Metabolic response classification using PERCIST criteria(22) showed 78% stable metabolic disease (SMD) and 22% progressive metabolic disease (PMD) rates in the control group; 64% SMD and 36% partial metabolic response (PMR) rates in the 5mg everolimus group; 50% SMD, and 50% PMR in the 10mg everolimus group (Fig. 2B).

**Anatomic Response—**Analysis for objective tumor shrinkage revealed a mean increase in tumor size in the control group and a dose-related reduction in tumor size in everolimus-treated patients; $p<0.001$; Figure 2C. In the control arm, 40% of patients met RECIST criteria definition for progression of disease (PD) while 60% had stable disease (SD); 18% of patients treated with 5mg everolimus had best response of PD while 82% achieved SD. Comparatively, 91% of patients in the 10mg everolimus group had SD and 9% met the RECIST criteria for partial response with 30% tumor shrinkage.

## Assessment of target modulation in tissue samples

Expression (immunoscore) of activated phosphorylated S6, p70S6K, eIF4E, AKT, mTOR and 4E-BP1 was determined by immunohistochemistry in a blinded fashion to provide a read-out of target modulation in the enrolled patients. Comparison of expression in baseline and post-treatment surgical samples were significantly different between the treated and control patients with regards to S6 (−36.06 (± 100.02), −13.69 (± 144.05), −77.03 (± 16.02;

p=0.071) and pS6 (−41.25 (± 65.62), −61.57 (± 35.8), −47.21 (± 44.96; p=0.063). There was a modest 3% reduction in p-p70S6K expression in control patients, but a 1–2 fold increase in treated patients (Table 3b). We, and others, have previously reported the paradoxical activation of p-AKT following inhibition of the mTORC1 complex with rapalogs in preclinical models *in vitro* and *in vivo*.(26, 27) The intensity of this paradoxical AKT activation is postulated to correlate with the degree of inhibition of mTORC2 kinase activity, thereby providing a direct measurement of the level of target engagement and pathway modulation. There was a low expression overall of pAKT and insufficient baseline tumor biopsy samples precluded accurate matched comparison. Nonetheless, pAKT immunoscore was overall higher in the post-treatment resected samples, with a stronger magnitude of increase noted for treated patients (supplementary Fig. S1). Unmatched mean immunoscore for nuclear and cytoplasmic pAKT staining increased more than 40-fold in the treated patients from 0.01 and 0.42 respectively at baseline to 4.4 and 2.34 post-treatment in the 10 mg cohort; and from 0.3 and 13.1 at baseline to 15 and 47.5 in the 5 mg cohort in comparison to 0.3 and 5.6 at baseline vs. 10.9 and 17.5 post-treatment in the control group. There was a significant negative correlation between metabolic response on PET imaging as measured by $SUV_{max}$ and percent change in immunoscore for nuclear p70S6K (R=−0.685; p=0.029) and cytoplasmic p70S6K (R=−0.664; p=0.036) expression in baseline and post-treatment; Table 3c and supplementary Figure S2. There was also a negative correlation between anatomic tumor shrinkage and changes in S6 expression (R=−0.520; p=0.069) and the ratio of pS6/S6 (R=−0.633; p=0.067); supplementary Figure S2.

## Genetic mutation analysis and correlation with metabolic response

SNaPshot multiplex sequencing was successfully performed in 28 of 33 baseline biopsy samples. Eight of the 28 samples revealed the presence of a genetic mutation including 6 cases (27%) with *K-Ras* mutation (G12C, G12D, G12V), and 1 case (4%) each of *N-Ras* (Q61L) and *EGFR* (L858R) mutated tumors. The 6 cases with *Ras* gene mutation were fortuitously enrolled either in the control or the everolimus (10mg) arm of the study. This enabled us to conduct a preliminary hypothesis-generating comparison of metabolic response based on the presence or absence of RAS gene mutation. Overall, there was a mean 17% increase in metabolic activity in *Ras* mutant tumors and a 12% reduction in non *Ras*-mutant tumors (p=0.203). When compared by treatment, *RAS*-mutant tumors in the control group had 88% increase in mean metabolic activity in comparison to an 30% reduction in the *RAS* mutant tumors treated with everolimus (p=0.218). Conversely, there was a 12% increase versus 21% reduction (p=0.039) respectively in metabolic activity of non-RAS mutant tumors in the control group and the everolimus (10mg) group (Fig. 2D).

## Sarcomatoid NSCLC response to single agent everolimus

One patient treated with 10mg everolimus for 3 weeks attained near complete metabolic response (74% reduction in $SUV_{max}$) and significant pathologic response with extensive necrosis observed in the resected tumor specimen, consistent with the PET findings (Fig. 3). The patient was a 69-year old Caucasian woman with approximately 20 pack-year smoking history. She had a biopsy-confirmed sarcomatoid variant of NSCLC and had a 3.6cm pathologic stage IB (pT2a, N0, M0) sarcomatoid NSCLC post-surgical resection. In order to elucidate potential genetic alterations responsible for the observed sensitivity of this patient

to everolimus, we compared the gene expression profile between the baseline and surgical resection specimen of her tumor with the profile from another patient with similar tumor histology who did not achieve significant metabolic response. We also employed SNaPshot targeted multiplex assay to asses for known driver mutations in EGFR, KRAS, NRAS, AKT, PI3K, IDH1, and HER2, as well as RNA-Seq technology to uncover novel mutations and fusion transcripts. The tumor content of the tissue employed for this analysis ranged between 35 and 60% cellularity. The responder had no detectable mutation in the targeted genes included in the SNaPshot panel. However, RNA-Seq deep sequencing and gene expression profile analysis revealed significant differences in the expression pattern of many genes. Supplementary Table S1 lists the top 1% of differentially expressed genes between the responding and the non responding patients. The full genomic data is available on the dbGAP database under the accession number phs000829.v1.p1 and is directly accessible at this URL: http://www.ncbi.nlm.nih.gov/projects/gap/cgibin/study.cgi?study_id=phs000829.v1.p1

One gene that was differentially expressed in the post-treatment sample compared to the baseline sample in the responder was the *BCL2L-11* gene that codes for BIM, which showed a 6-fold increase in expression (Fig. 3). There was insufficient pretreatment tissue sample in the majority of cases, including the index case, to conduct IHC to assess baseline BIM expression for this post-hoc analysis. However, analysis in available post-treatment samples revealed that BIM expression immunoscore was nearly 2-fold higher in treated patients compared to control patients (84.3 for 5mg everolimus; 80.5 for 10mg everolimus vs. 48.6 for control). Moreover, there was a correlation of high BIM expression with a greater reduction in metabolic activity on paired PET scan (Table 3c; Pearson correlation coefficient: −0.390; p=0.073 and supplementary Fig. S2).

## Discussion

This phase IB window-of-opportunity study demonstrated robust biological effects of everolimus in a cohort of early stage NSCLC patients. These patients had not received prior systemic anti-cancer therapy and we were thus able to assess the effect of everolimus on the natural cancer cell phenotype unaltered by compensatory genetic and molecular adaptations induced by systemic anticancer therapy. The common practice of first testing novel investigational agents in heavily pretreated patients might confounds the ability to demonstrate the expected clinical efficacy because prior therapies induce cellular adaptations, some of which might not be critical for the natural development and progression of cancer, but can nonetheless impact the biological activity of the anticancer agent.(28) This limitation is especially germane to the current strategy of precision medicine, where accurate replication of the preclinical model is required for successful clinical demonstration of targeted agent efficacy.

Our study demonstrates the safety, feasibility and biologic advantages of ‘window of opportunity’ studies in patients with early stage NSCLC. More than 90% of enrolled patients completed the planned interventions and proceeded to successful surgical resection, similar to the experience in the preoperative study of pazopanib in early stage lung cancer patients where 86% of enrolled patients completed the intervention and proceeded to surgery.(29)

Furthermore, our study demonstrates the willingness of newly diagnosed lung cancer patients to participate in this type of trial, with 33 (74%) of 45 patients screened consenting to participate, despite understandable concerns regarding potential delay in initiating treatment. Our results successfully addressed several key aspects of mTOR inhibitor efficacy in general and specifically in lung cancer patients. Although everolimus is approved at both the 5 and 10mg doses for various indications,(19, 20) we showed that the 5mg dose was less potent than the 10mg dose in modulating key signaling proteins in the PI3K/AKT/mTOR pathway and in inducing metabolic response or anatomic tumor shrinkage. The 10mg dose of everolimus induced a stronger p-AKT expression concomitant with greater reduction in the downstream read-outs of pathway inhibition in comparison to the 5mg dose, suggesting that the higher dose is the optimal choice to employ for efficacy studies, at least in patients with NSCLC. It is noteworthy that nearly all the previous trials of everolimus in lung cancer recommended or utilized the 5mg dose. This potentially suboptimal dose selection could also have contributed to the failure of these early phase studies to demonstrate significant clinical benefit that could justify further testing of everolimus in lung cancer.(4, 6, 9, 11, 30) Interestingly, a dose response trend was observed in a phase IB study of everolimus when combined with paclitaxel in advanced small cell lung cancer,(7) similar to our findings of superior metabolic and anatomic tumor response with the 10mg dose of everolimus.

Detailed characterization of patients who achieved unexpected clinical benefit of novel agents is a well-honed research paradigm that has led to the identification of molecular subsets of lung cancer such as EGFR mutant and ALK- or ROS1-gene rearranged lung cancer.(31–33) Similarly, TSC1 mutation was identified as a sensitizing genetic aberration in a bladder cancer patient with an unexpected completed response to treatment with everolimus.(34) Sarcomatoid variant of NSCLC is a particularly aggressive disease with very poor clinical outcomes. The exquisite sensitivity of a patient with sarcomatoid NSCLC to a short duration of treatment with single agent everolimus prompted the detailed characterization of the molecular and genetic phenotype of the tumor. We observed a 6-fold increased expression of the *BCL2L-11* gene that codes for BIM protein, a pro-apoptotic member of the Bcl2 protein family. Preclinical models of kinase addicted cancers such as Bcr-abl-addicted leukemia, EGFR mutant lung cancer and HER2 kinase-addicted breast cancers demonstrated that activated BIM is required for apoptosis and clinical efficacy of these inhibitors.(35–39) Furthermore, baseline BIM protein expression was shown to be a strong predictor of efficacy of kinase inhibitors including agents targeting the mTOR pathway.(35) Indeed, a deletion polymorphism in the *BCL2L-11* gene resulting in preferential transcription of the non BH3-containing splice variant of BIM, which is incapable of activating the apoptosis cascade, has also been implicated in de novo resistance to kinase inhibitors.(40) Mechanistic interrogation of BIM and other Bcl2 family proteins in relation to mTOR inhibitor sensitivity in lung cancer cell lines is currently ongoing in our lab to further explore this finding.

*KRAS* gene activation resulting from exon 12 coding sequence mutation has been shown to negatively impact the efficacy of PI3K/mTOR pathway targeted agents in preclinical animal models and was therefore proposed as a potential biomarker in human subjects.(41, 42) In a

preliminary comparison of metabolic changes in the six patients with *RAS* mutant tumors to those with non-*RAS* mutant tumors in our patient population, we observed similar degree of modulation by FDG-PET imaging. While this insufficient to conclude that mTOR inhibitor is clinically effective in RAS mutant tumors, potential explanations for this observation include the possibility that our patients harbor other genetic alterations not included in our mutation screen panel. One such example is loss of *LKB1* gene, which is present in approximately 30% of patients with adenocarcinoma subtype of NSCLC (3, 43) and whose co-occurrence with *KRAS* mutation was shown to preserve the sensitivity of *KRAS*-mutant cell lines to mTOR-targeted agents.(42) Additionally, our approach of evaluating the efficacy of everolimus in previously untreated subjects could have allowed us to observe this activity of everolimus in KRAS-mutant tumors similar to other published reports of mTOR inhibitor activity in previously untreated lung cancer tumors harboring the G12F *KRAS* mutation.(11) In conclusion, using the window of opportunity platform, tissue-based analysis and metabolic imaging, we established that the 10mg dose of everolimus modulated the targets more effectively than the lower dose of 5mg in NSCLC. Future evaluation of this agent in lung cancer should strive to use the maximum dose of 10mg of everolimus to ensure optimal biological effect.

## Supplementary Material

Refer to Web version on PubMed Central for supplementary material.

## Acknowledgments

**Funding:** National Institute of Health program project grant P01 CA116676 and 3P01 CA116676-05S1 (FRK); Department of Defense Grant Award W81XWH-05-2-0027 (FRK) and Distinguished Cancer Researcher Award from Georgia Research Alliance (TKO, SSR, GLS, SS, FRK). Novartis Oncology generously provided Everolimus to all patients.

We thank Jaqueline Rogerio and John Hohneker for their assistance with pharmaceutical support for the study. We thank Anthea Hammond, PhD for editorial assistance, Charles Butler, BA for his role in tissue sample collection from patients and Dianne Alexis, MSC for her role in performing the immunohistochemical staining.

## References

1. Tsao AS, McDonnell T, Lam S, Putnam JB, Bekele N, Hong WK, et al. Increased phospho-AKT (Ser(473)) expression in bronchial dysplasia: implications for lung cancer prevention studies. Cancer epidemiology, biomarkers & prevention : a publication of the American Association for Cancer Research, cosponsored by the American Society of Preventive. Oncology. 2003; 12:660–4.
2. Balsara BR, Pei J, Mitsuuchi Y, Page R, Klein-Szanto A, Wang H, et al. Frequent activation of AKT in non-small cell lung carcinomas and preneoplastic bronchial lesions. Carcinogenesis. 2004; 25:2053–9. [PubMed: 15240509]
3. Sanchez-Cespedes M, Parrella P, Esteller M, Nomoto S, Trink B, Engles JM, et al. Inactivation of LKB1/STK11 is a common event in adenocarcinomas of the lung. Cancer Res. 2002; 62:3659–62. [PubMed: 12097271]
4. Ramalingam SS, Owonikoko TK, Behera M, Subramanian J, Saba NF, Kono SA, et al. Phase II study of docetaxel in combination with everolimus for second- or third-line therapy of advanced non-small-cell lung cancer. Journal of thoracic oncology : official publication of the International Association for the Study of Lung Cancer. 2013; 8:369–72.
5. Milton DT, Riely GJ, Azzoli CG, Gomez JE, Heelan RT, Kris MG, et al. Phase 1 trial of everolimus and gefitinib in patients with advanced nonsmall-cell lung cancer. Cancer. 2007; 110:599–605. [PubMed: 17577220]

6. Papadimitrakopoulou VA, Soria JC, Jappe A, Jehl V, Klimovsky J, Johnson BE. Everolimus and erlotinib as second- or third-line therapy in patients with advanced non-small-cell lung cancer. Journal of thoracic oncology : official publication of the International Association for the Study of Lung Cancer. 2012; 7:1594–601.
7. Sun JM, Kim JR, Do IG, Lee SY, Lee J, Choi YL, et al. A phase-1b study of everolimus plus paclitaxel in patients with small-cell lung cancer. British journal of cancer. 2013
8. Vansteenkiste J, Solomon B, Boyer M, Wolf J, Miller N, Di Scala L, et al. Everolimus in combination with pemetrexed in patients with advanced non-small cell lung cancer previously treated with chemotherapy: a phase I study using a novel, adaptive Bayesian dose-escalation model. Journal of thoracic oncology : official publication of the International Association for the Study of Lung Cancer. 2011; 6:2120–9.
9. Riely GJ, Kris MG, Zhao B, Akhurst T, Milton DT, Moore E, et al. Prospective assessment of discontinuation and reinitiation of erlotinib or gefitinib in patients with acquired resistance to erlotinib or gefitinib followed by the addition of everolimus. Clinical cancer research : an official journal of the American Association for Cancer Research. 2007; 13:5150–5. [PubMed: 17785570]
10. Ramalingam SS, Harvey RD, Saba N, Owonikoko TK, Kauh J, Shin DM, et al. Phase 1 and pharmacokinetic study of everolimus, a mammalian target of rapamycin inhibitor, in combination with docetaxel for recurrent/refractory nonsmall cell lung cancer. Cancer. 2010; 116:3903–9. [PubMed: 20564143]
11. Price KA, Azzoli CG, Krug LM, Pietanza MC, Rizvi NA, Pao W, et al. Phase II trial of gefitinib and everolimus in advanced non-small cell lung cancer. Journal of thoracic oncology : official publication of the International Association for the Study of Lung Cancer. 2010; 5:1623–9.
12. Baselga J, Campone M, Piccart M, Burris HA 3rd, Rugo HS, Sahmoud T, et al. Everolimus in postmenopausal hormone-receptor-positive advanced breast cancer. The New England journal of medicine. 2012; 366:520–9. [PubMed: 22149876]
13. Yao JC, Shah MH, Ito T, Bohas CL, Wolin EM, Van Cutsem E, et al. Everolimus for advanced pancreatic neuroendocrine tumors. The New England journal of medicine. 2011; 364:514–23. [PubMed: 21306238]
14. Motzer RJ, Escudier B, Oudard S, Hutson TE, Porta C, Bracarda S, et al. Efficacy of everolimus in advanced renal cell carcinoma: a double-blind, randomised, placebo-controlled phase III trial. Lancet. 2008; 372:449–56. [PubMed: 18653228]
15. Owonikoko TK, Khuri FR. Targeting the PI3K/AKT/mTOR Pathway. American Society of Clinical Oncology educational book / ASCO American Society of Clinical Oncology Meeting. 2013; 2013:395–401.
16. Boulay A, Zumstein-Mecker S, Stephan C, Beuvink I, Zilbermann F, Haller R, et al. Antitumor efficacy of intermittent treatment schedules with the rapamycin derivative RAD001 correlates with prolonged inactivation of ribosomal protein S6 kinase 1 in peripheral blood mononuclear cells. Cancer Res. 2004; 64:252–61. [PubMed: 14729632]
17. Nogova L, Boellaard R, Kobe C, Hoetjes N, Zander T, Gross SH, et al. Downregulation of 18F-FDG uptake in PET as an early pharmacodynamic effect in treatment of non-small cell lung cancer with the mTOR inhibitor everolimus. Journal of nuclear medicine : official publication, Society of Nuclear Medicine. 2009; 50:1815–9.
18. Honer M, Ebenhan T, Allegrini PR, Ametamey SM, Becquet M, Cannet C, et al. Anti-Angiogenic/Vascular Effects of the mTOR Inhibitor Everolimus Are Not Detectable by FDG/FLT-PET. Translational oncology. 2010; 3:264–75. [PubMed: 20689768]
19. O'Donnell A, Faivre S, Burris HA 3rd, Rea D, Papadimitrakopoulou V, Shand N, et al. Phase I pharmacokinetic and pharmacodynamic study of the oral mammalian target of rapamycin inhibitor everolimus in patients with advanced solid tumors. J Clin Oncol. 2008; 26:1588–95. [PubMed: 18332470]
20. Tabernero J, Rojo F, Calvo E, Burris H, Judson I, Hazell K, et al. Dose- and schedule-dependent inhibition of the mammalian target of rapamycin pathway with everolimus: a phase I tumor pharmacodynamic study in patients with advanced solid tumors. J Clin Oncol. 2008; 26:1603–10. [PubMed: 18332469]
21. Kovarik JM, Eisen H, Dorent R, Mancini D, Vigano M, Rouilly M, et al. Everolimus in de novo cardiac transplantation: pharmacokinetics, therapeutic range, and influence on cyclosporine

exposure. The Journal of heart and lung transplantation : the official publication of the International Society for Heart Transplantation. 2003; 22:1117–25.

22. Wahl RL, Jacene H, Kasamon Y, Lodge MA. From RECIST to PERCIST: Evolving Considerations for PET response criteria in solid tumors. Journal of nuclear medicine : official publication, Society of Nuclear Medicine. 2009; 50 (Suppl 1):122S–50S.
23. Brignol N, McMahon LM, Luo S, Tse FL. High-throughput semi-automated 96-well liquid/liquid extraction and liquid chromatography/mass spectrometric analysis of everolimus (RAD 001) and cyclosporin a (CsA) in whole blood. Rapid communications in mass spectrometry : RCM. 2001; 15:898–907. [PubMed: 11400194]
24. Detre S, Saclani Jotti G, Dowsett M. A “quickscore” method for immunohistochemical semiquantitation: validation for oestrogen receptor in breast carcinomas. J Clin Pathol. 1995; 48:876–8. [PubMed: 7490328]
25. Su Z, Dias-Santagata D, Duke M, Hutchinson K, Lin YL, Borger DR, et al. A platform for rapid detection of multiple oncogenic mutations with relevance to targeted therapy in non-small-cell lung cancer. The Journal of molecular diagnostics : JMD. 2011; 13:74–84. [PubMed: 21227397]
26. Sun SY, Rosenberg LM, Wang X, Zhou Z, Yue P, Fu H, et al. Activation of Akt and eIF4E survival pathways by rapamycin-mediated mammalian target of rapamycin inhibition. Cancer Res. 2005; 65:7052–8. [PubMed: 16103051]
27. O’Reilly KE, Rojo F, She QB, Solit D, Mills GB, Smith D, et al. mTOR inhibition induces upstream receptor tyrosine kinase signaling and activates Akt. Cancer Res. 2006; 66:1500–8. [PubMed: 16452206]
28. Sequist LV, Waltman BA, Dias-Santagata D, Digumarthy S, Turke AB, Fidias P, et al. Genotypic and histological evolution of lung cancers acquiring resistance to EGFR inhibitors. Sci Transl Med. 2011; 3:75ra26.
29. Altorki N, Lane ME, Bauer T, Lee PC, Guarino MJ, Pass H, et al. Phase II proof-of-concept study of pazopanib monotherapy in treatment-naive patients with stage I/II resectable non-small-cell lung cancer. J Clin Oncol. 2010; 28:3131–7. [PubMed: 20516450]
30. Tarhini A, Kotsakis A, Gooding W, Shuai Y, Petro D, Friedland D, et al. Phase II study of everolimus (RAD001) in previously treated small cell lung cancer. Clinical cancer research : an official journal of the American Association for Cancer Research. 2010; 16:5900–7. [PubMed: 21045083]
31. Bergethon K, Shaw AT, Ou SH, Katayama R, Lovly CM, McDonald NT, et al. ROS1 rearrangements define a unique molecular class of lung cancers. J Clin Oncol. 2012; 30:863–70. [PubMed: 22215748]
32. Lynch TJ, Bell DW, Sordella R, Gurubhagavatula S, Okimoto RA, Brannigan BW, et al. Activating mutations in the epidermal growth factor receptor underlying responsiveness of non-small-cell lung cancer to gefitinib. The New England journal of medicine. 2004; 350:2129–39. [PubMed: 15118073]
33. Soda M, Choi YL, Enomoto M, Takada S, Yamashita Y, Ishikawa S, et al. Identification of the transforming EML4-ALK fusion gene in non-small-cell lung cancer. Nature. 2007; 448:561–6. [PubMed: 17625570]
34. Iyer G, Hanrahan AJ, Milowsky MI, Al-Ahmadie H, Scott SN, Janakiraman M, et al. Genome sequencing identifies a basis for everolimus sensitivity. Science. 2012; 338:221. [PubMed: 22923433]
35. Faber AC, Corcoran RB, Ebi H, Sequist LV, Waltman BA, Chung E, et al. BIM expression in treatment-naive cancers predicts responsiveness to kinase inhibitors. Cancer discovery. 2011; 1:352–65. [PubMed: 22145099]
36. Kuroda J, Puthalakath H, Cragg MS, Kelly PN, Bouillet P, Huang DC, et al. Bim and Bad mediate imatinib-induced killing of Bcr/Abl+ leukemic cells, and resistance due to their loss is overcome by a BH3 mimetic. Proc Natl Acad Sci U S A. 2006; 103:14907–12. [PubMed: 16997913]
37. Kuribara R, Honda H, Matsui H, Shinjyo T, Inukai T, Sugita K, et al. Roles of Bim in apoptosis of normal and Bcr-Abl-expressing hematopoietic progenitors. Molecular and cellular biology. 2004; 24:6172–83. [PubMed: 15226421]

38. Cragg MS, Kuroda J, Puthalakath H, Huang DC, Strasser A. Gefitinib-induced killing of NSCLC cell lines expressing mutant EGFR requires BIM and can be enhanced by BH3 mimetics. PLoS medicine. 2007; 4:1681–89. discussion 90. [PubMed: 17973573]

39. Costa DB, Halmos B, Kumar A, Schumer ST, Huberman MS, Boggon TJ, et al. BIM mediates EGFR tyrosine kinase inhibitor-induced apoptosis in lung cancers with oncogenic EGFR mutations. PLoS medicine. 2007; 4:1669–79. discussion 80. [PubMed: 17973572]

40. Ng KP, Hillmer AM, Chuah CT, Juan WC, Ko TK, Teo AS, et al. A common BIM deletion polymorphism mediates intrinsic resistance and inferior responses to tyrosine kinase inhibitors in cancer. Nat Med. 2012; 18:521–8. [PubMed: 22426421]

41. Engelman JA, Chen L, Tan X, Crosby K, Guimaraes AR, Upadhyay R, et al. Effective use of PI3K and MEK inhibitors to treat mutant Kras G12D and PIK3CA H1047R murine lung cancers. Nat Med. 2008; 14:1351–6. [PubMed: 19029981]

42. Mahoney CL, Choudhury B, Davies H, Edkins S, Greenman C, Haaften G, et al. LKB1/KRAS mutant lung cancers constitute a genetic subset of NSCLC with increased sensitivity to MAPK and mTOR signalling inhibition. British journal of cancer. 2009; 100:370–5. [PubMed: 19165201]

43. Ji H, Ramsey MR, Hayes DN, Fan C, McNamara K, Kozlowski P, et al. LKB1 modulates lung cancer differentiation and metastasis. Nature. 2007; 448:807–10. [PubMed: 17676035]

## Statement of translational significance

This window-of-opportunity phase IB clinical trial studied the pharmacodynamic changes induced by everolimus in previously untreated, resectable non small cell lung cancer. Using a combination of in vivo and ex vivo assessments with FDG PET, immunohistochemistry and genomic assays, we carefully assessed for evidence of mTOR pathway perturbation in patients treated with an allosteric mTOR inhibitor. Key findings from this work such as a dose-dependent biologic effect of everolimus and the near complete metabolic and pathologic response in a case of sarcomatoid lung cancer provide translational insight that will guide future development of this class of agents not only in lung cancer but in other tumor types. Additionally, metabolic response and anatomic tumor shrinkage observed in a significant proportion of patients following a short of duration of therapy with everolimus suggests potential clinical utility of this agent in well-selected lung cancer patients.

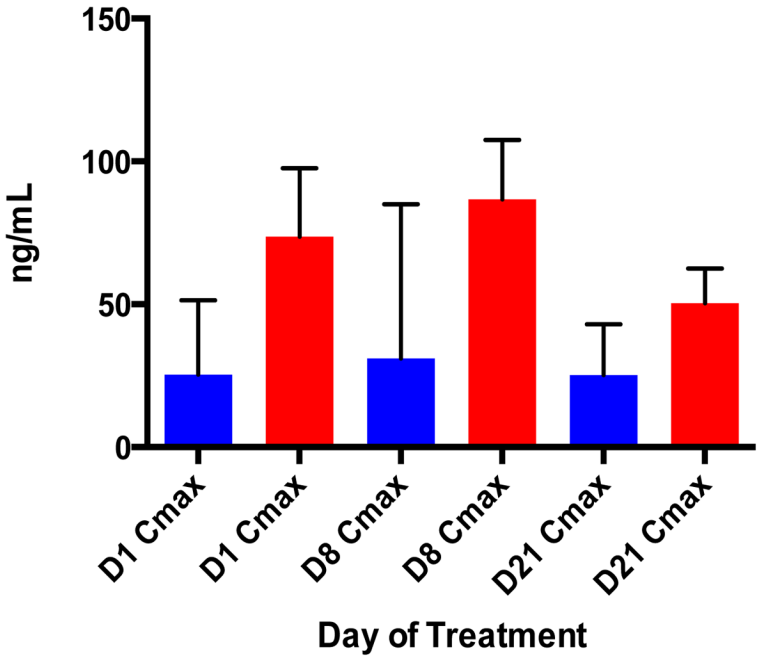


**Fig. 1.**

Everolimus pharmacokinetic characteristics. Bar graphs showing a dose proportional increase in maximum concentration ($C_{max}$) of everolimus measured in whole blood on Days 1, 8 and 21. Blue and red bars represent the 5 mg and 10 mg doses of everolimus, respectively.

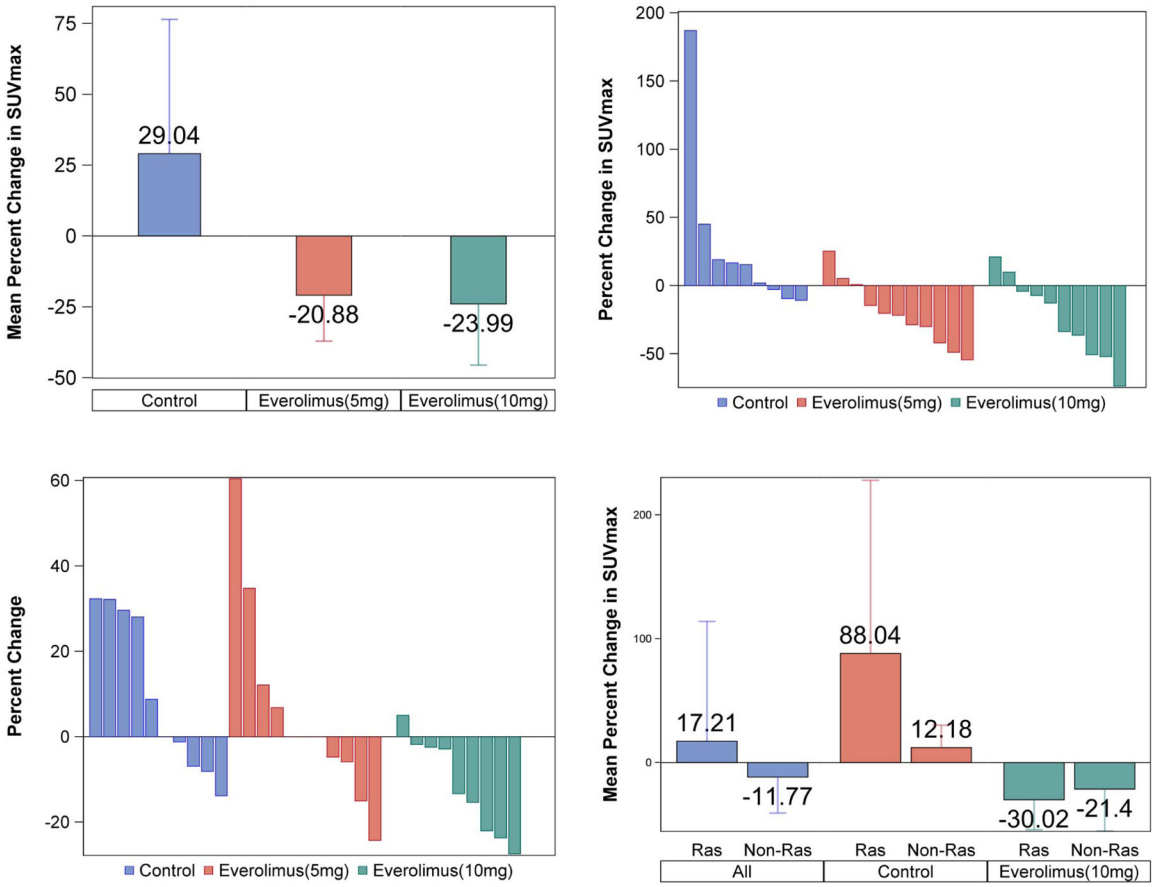


**Fig. 2.**

Clockwise from top left:

A: Percent change in maximum standardized uptake value (SUVmax) on paired PET/CT imaging in different patient groups with reduced metabolic activity in everolimus-treated patients and increased activity in the control group.

B: Percent change in metabolic activity (measured as SUVmax). Waterfall plot of percent change in SUVmax on paired PET imaging for individual patients according to treatment group (C=control; E5=Everolimus 5 mg; E10=Everolimus 10 mg).

C: Waterfall plot of change in tumor size (measured as maximum tumor diameter) for individual patients by treatment group (C=control; E5=Everolimus 5 mg; E10=Everolimus 10 mg).

D: Changes in metabolic activity on paired PET imaging by RAS gene mutation status showing comparable activity of everolimus (10mg) in RAS mutant and non mutant tumors.

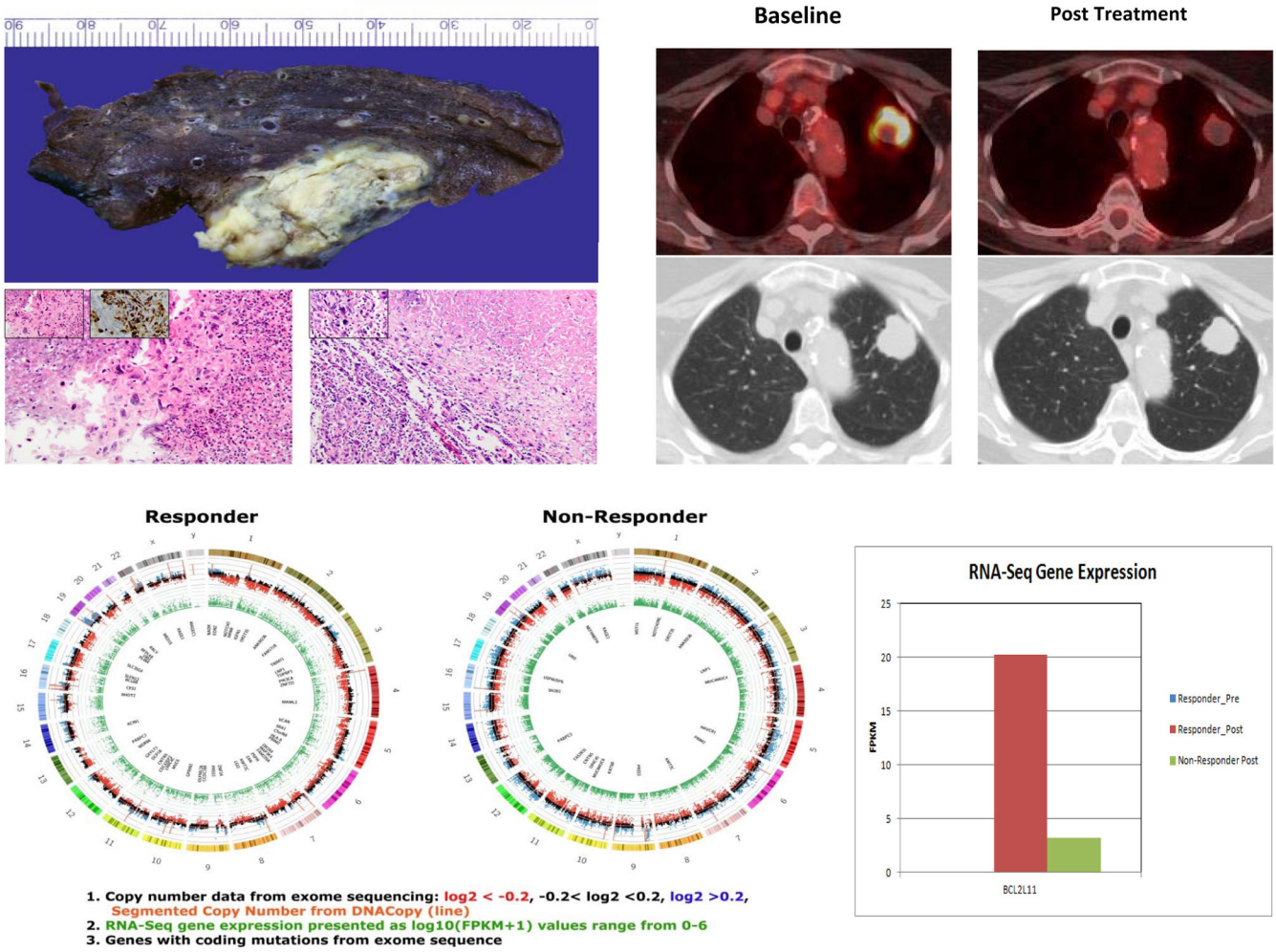


**Fig. 3.**

Major pathologic response and near complete metabolic response in a patient with poorly differentiated, sarcomatoid NSCLC following 4 weeks of everolimus at 10mg daily dose. Left upper panel showing coagulative tumor necrosis in the resected specimen along with histologic sections from base line biopsy (left, 200×) and post-treatment surgical sections (right, 100×) from a patient with near complete metabolic response to everolimus (10mg daily for 21 days). Note the extensive tumor necrosis in the post treatment section. Insets showing sarcomatoid cellular morphology (400×) and positive pancytokeratin staining (400×) on immunohistochemistry. Right upper panel: Baseline (left) and post-treatment (right) FDG-PET and corresponding CT scan images showing near complete metabolic response in a sarcomatoid NSCLC patient treated with everolimus. Lower panel: Circos plots of exome and whole transcriptome RNA-seq of the post-treatment sample from the patient with near complete metabolic and pathologic response and another patient with sarcomatoid tumor that did not respond to everolimus (Non-Responder). 1. Outer circle depicts copy number derived from exome sequencing. The log2 ratio of total reads per exon divided by median reads across all samples, are shown on a Y-axis ranging from −1 to 1.5. Reads with log2 ratio of < −0.2 are red, those with log2 ratio of > 0.2 are blue and those

between −0.2 and 0.2 are black. An orange line of the segmented copy number generated using the DNACopy algorithm overlays this data. 2. Green inner ring shows RNA-Seq gene expression presented as log10 (FPKM+1) values range from 0–6. 3. The inner circle, lists genes with coding mutations identified by exome sequence. Mutations had to be exonic, non-synonymous, indel or splice site mutation that had at least 20× coverage with >10% variant reads. This list was parsed to exclude SNPs, SNV that were not >1% of EVS or 1000 genomes, not in 100% of reads, and had to have a COSMIC ID. The full genomic data is available on the dbGAP database under the accession number phs000829.v1.p1 and is directly accessible at this URL: http://www.ncbi.nlm.nih.gov/projects/gap/cgibin/study.cgi?study_id=phs000829.v1.p1

## Table 1

Patient demographics, tumor characteristics and treatment assignment. Details of patient demographics and characteristics of the tumors according to final pathologic staging and the distribution of patients to control and treatment arms of the study.

| Variable | Subgroup | N (%) |
|---|---|---|
| Race | African American | 9 (27.27) |
| | Caucasian | 24 (72.73) |
| Age at enrollment | Mean (± SD) | 62 (± 9) |
| | Median (Range) | 64 (36 – 77) |
| Gender | Female | 19 (57.58) |
| | Male | 14(42.42) |
| Histology | Adenocarcinoma | 22 (66.67) |
| | Others | 4 (12.12) |
| | Squamous | 7 (21.21) |
| Stage | I | 14 (42.42) |
| | II | 13 (39.39) |
| | III | 6 (18.18) |
| Treatment Groups | Control | 10 (30.3) |
| | Everolimus (5mg) | 12 (36.36) |
| | Everolimus (10mg) | 11 (33.33) |

Total N=33. Data are presented as number of patients (%), mean (± SD) or median (range).

## Table 2

Treatment-emergent adverse events

Summary of the most frequent adverse events graded according to CTCAE version 3 in patients treated with everolimus.

| Adverse event | Grade 2 | Grade 3 | Grade 4 |
|---|---|---|---|
| Cough | 1 | | |
| Elevated Cholesterol | 1 | | |
| Elevated Creatinine | 1 | | |
| Weight-loss | 1 | | |
| Elevated Alkaline Phosphatase | 1 | | |
| Anemia | 3 | | |
| Hypophosphatemia | 3 | | |
| Hypertriglyceridemia | 6 | | |
| Mouth Sores | 1 | | |
| Sore Throat | 1 | | |
| Rash | 3 | | |
| Upper respiratory infection | 1 | | |
| Sinusitis | 2 | | |
| Hypercalcemia | 1 | | |
| Urinary frequency | 1 | | |
| Pain | 1 | 1 | |
| Hypoalbuminemia | 1 | 2 | |
| Hyperglycemia | 3 | 1 | |
| Fatigue | 2 | 1 | |
| Hypokalemia | 1 | 2 | |
| Chest pain | 1 | 1 | 1 |
| Edema | 1 | | |
| Hyponatremia | 5 | | |
| Diarrhea | 1 | | |
| Respiratory failure | | 3 | |
| MRSA Bacteremia | | 1 | |
| Acute renal failure | | 1 | |

## Table 3a
### Everolimus pharmacokinetic analysis parameters

Pharmacokinetic analysis showing dose proportional increase in $C_{min}$, $C_{max}$ and AUC of everolimus when comparing the 5mg to the 10mg dose.

| **Parameter*** | **5 mg (n=12)** | **10 mg (n=7)** |
|---|---|---|
| $T_{max}$ (hr.) | 2 (1 – 2) | 2 (1 – 2) |
| Day 1 $C_{max}$ (ng/mL) | 29.2 ± 9.9 | 61.8 ± 26.1 |
| Day 8 $C_{min}$ (ng/mL) | 6.3 ± 2.9 | 17.8 ± 7.6 |
| Day 8 $C_{max}$ (ng/mL) | 42.1 ± 17.2 | 81.8 ± 22.8 |
| Day 21 $C_{min}$ (ng/mL) | 5.7 ± 2.3 | 13.7 ± 9.2 |
| Day 21 $C_{max}$ (ng/mL) | 35 ± 15.9 | 51.5 ± 9.9 |
| Day 8 $AUC_{0-24}$ (ng.hr/mL) | 210.8 ± 75.9 | 578.7 ± 186.5 |
| Day 21 $AUC_{0-24}$ (ng.hr/mL) | 204.7 ± 87.4 | 506.5 ± 207.6 |

**Table 3b**

Tissue-based analysis of mTOR pathway protein modulation

| Parameter | Overall percent change for all patients | P-value * | Dose of Everolimus | | | P-value† | P-value ‡ |
|---|---|---|---|---|---|---|---|
| | | | 0 | 5 | 10 | | |
| S6 | −49.21 (± 86.59) | **0.045** | −36.06 (± 100.02) | −13.69 (± 144.05) | −77.03 (± 16.02) | 0.510 | **0.071** |
| pS6 | −48.59 (± 46.7) | **0.002** | −41.25 (± 65.62) | −61.57 (± 35.8) | −47.21 (± 44.96) | 0.866 | **0.063** |
| pS6/S6 | 62.85 (± 208.1) | 0.365 | −85.75 (± 20.15) | −100 (±NA) | 128.57 (± 219.26) | 0.350 | 0.297 |
| pMTOR | −17.42 (± 113.57) | 0.622 | −6.58 (± 138.88) | 30 (± 153.95) | −63.82 (± 51.3) | 0.592 | 0.608 |
| p4E-BP1 | −56.39 (± 84.35) | 0.101 | −95.37 (± 4.24) | 150 (±NA) | −78.75 (± 14.36) | **<.001** | 0.564 |
| p70s6k | 55.17 (± 312.26) | 0.633 | 25 (± 176.78) | 137.14 (± 442.07) | −78.62 (± 22.79) | 0.780 | 0.757 |
| p70s6k Cytoplasmic | 161.44 (± 513.8) | 0.322 | −19.17 (± 73.16) | 0.56 (± 14.93) | 305.37 (± 686.3) | 0.645 | 0.459 |
| p70s6k Nuclear | 145.51 (± 329.17) | 0.173 | −3.33 (± 100.17) | 135 (± 49.5) | 223.43 (± 437.7) | 0.670 | 0.158 |
| pe1f4e | −22.88 (± 49.67) | 0.139 | −50 (± 86.6) | 2.78 (± 5.56) | −27.13 (± 42.17) | 0.406 | 0.220 |
| PAKT Nuclear | −16.67 (± 40.82) | 0.363 | −33.33 (± 57.74) | NA | 0 (± 0) | 0.374 | 0.850 |
| PAKT Cytoplasmic | 87.5 (± 331.39) | 0.480 | 200 (± 469.04) | NA | −25 (± 50) | 0.377 | 0.505 |
| Bim | −19.26 (± 49.3) | 0.492 | −11.76 (±NA) | NA | −21.76 (± 60.07) | 0.899 | 0.766 |

Changes in the expression level of phosphorylated forms of key protein molecules in the mTOR signaling pathway and the proapoptotic protein BIM (measured as percent change in immunoscore between post-treatment samples relative to baseline) between baseline and surgical resection specimens.

Data are presented as mean (±SD).

* P-value is calculated by T-test for the percent change.

† P-value is calculated by ANOVA for the percent change.

‡ P-value is calculated by ANOVA for absolute values for pre- and post-measurements.

NA Not Available

## Table 3c

Correlation of tissue-based PD biomarkers and metabolic changes on PET There was negative correlation between p70S6K (cytoplasmic and nuclear) and changes in metabolic activity on PET imaging. BIM expression in resected post treatment surgical specimen also showed a modest negative correlation with percent change in SUVmax on PET imaging (p-value=0.073).

| Variable | Pearson CC | P-value |
|---|---|---|
| S6 | 0.451 | 0.106 |
| pS6 | 0.181 | 0.555 |
| pS6/S6 | −0.038 | 0.917 |
| pMTOR | −0.140 | 0.699 |
| p4E-BP1 | 0.353 | 0.437 |
| p70s6k | 0.154 | 0.742 |
| p70s6k Cytoplasmic | −0.664 | **0.036** |
| p70s6k Nuclear | −0.685 | **0.029** |
| pe1f4e | 0.396 | 0.229 |
| PAKT Cytoplasmic | 0.252 | 0.585 |
| BIM Immunoscore | −0.318 | 0.682 |
| BIM expression in post-treatment samples | −0.390 | **0.073** |